



Ytterbium-Centered Isotopic Enrichment Leading to a Zero-Field Single-Molecule Magnet

Jessica Flores Gonzalez, Haiet Douib, Boris Le Guennic, Fabrice Pointillart,
Olivier Cador

► To cite this version:

Jessica Flores Gonzalez, Haiet Douib, Boris Le Guennic, Fabrice Pointillart, Olivier Cador. Ytterbium-Centered Isotopic Enrichment Leading to a Zero-Field Single-Molecule Magnet. *Inorganic Chemistry*, 2021, 60 (2), pp.540-544. 10.1021/acs.inorgchem.0c02652 . hal-03128537

HAL Id: hal-03128537

<https://hal.science/hal-03128537v1>

Submitted on 22 Feb 2021

HAL is a multi-disciplinary open access archive for the deposit and dissemination of scientific research documents, whether they are published or not. The documents may come from teaching and research institutions in France or abroad, or from public or private research centers.

L'archive ouverte pluridisciplinaire **HAL**, est destinée au dépôt et à la diffusion de documents scientifiques de niveau recherche, publiés ou non, émanant des établissements d'enseignement et de recherche français ou étrangers, des laboratoires publics ou privés.

Ytterbium centered isotopic enrichment leads to zero-field Single Molecule Magnet

Jessica Flores Gonzalez,^a Haiet Douib,^a Boris Le Guennic,^a Fabrice Pointillart,^{*a} Olivier Cador^{*a}

^a Univ Rennes, CNRS, ISCR (Institut des Sciences Chimiques de Rennes) - UMR 6226, 35000 Rennes, France

Dedicated to Dr. Jean-René Hamon for his 65th anniversary

ABSTRACT An unprecedented combination of isotopic enrichment and magnetic dilution approaches for a prolate ytterbium(III) based complex was performed. It results in the appearance of both first observations of nuclear spin effect on Quantum Tunneling of the Magnetization and slow magnetic relaxation for an ytterbium complex under zero applied field.

A tremendous work has been performed in the last two decades to improve the properties of Single-Molecule Magnets (SMMs).¹ Since the pioneering work of Ishikawa *et al.*,² who reported the first mononuclear lanthanide-based SMM, the blocking temperatures of such nanomagnets never stop to increase reaching recently liquid nitrogen temperature.³ The recent developments stand on the disposition of negatively charged ligands around lanthanide ions depending on their prolate or oblate character (along an axis for oblate and in a plane for prolate)^{1a} to stabilize the largest M_J components (axial anisotropy). The demonstration in the oblate case (Dy^{III}) is spectacular³ but less obvious in the prolate case. There are some examples of SMMs of Yb^{III} in the literature⁴ but in most cases, the slow relaxation of the magnetic moment is visible only under an applied constant field. $K_{13}[Yb(\beta 2-SiW_{11}O_{39})_2] \cdot xH_2O$, published by M. A. AlDamen *et al.*,^{4b} is the only member that shows the beginning of a slowing down of the relaxation of the magnetic moment in zero applied magnetic field. One should mention that in this latter case the ground state is characterized by the Kramers doublet $M_J = \pm 5/2$ of the $^2F_{7/2}$ multiplet ground state, and so, that it is not necessary to stabilize the highest M_J state to promote SMM behavior. The main reason that hinders slow relaxation of the magnetization in Yb^{III} -based complexes (beside the stabilization of large M_J states) is probably the domination of the Quantum Tunneling of the Magnetization (QTM) at low temperature, that is due for Kramers ions, to the perturbation of the electronic magnetic moment by local magnetic field. Dipolar interactions (intermolecular) on one side and hyperfine interactions (intramolecular) on the other side can be responsible of such local field. Magnetic dilution decreases intermolecular dipolar interaction and slows down relaxation⁵ and isotopic enrichment at lanthanide site diminishes if $I=0$ ^{6,7} or increases if $I \neq 0$ ^{7,8} hyperfine interactions that slows down or accelerates, respectively, the relaxation.

Some of us reported investigations on $[Dy(tta)_3(L)] \cdot C_6H_{14}$ ($tta = 2$ -thenoyltrifluoroacetate and $L = 4,5$ -bis(propylthio)-tetrathiafulvalene-2-(2-pyridyl) benzimidazole methyl-2-pyridine)⁹ in which the relaxation time has been multiplied by ten thousand at 2 K in cancelling the effect of hyperfine coupling and dipolar interactions^{6a,8}. In this case, the natural Dysprosium derivative is clearly a SMM in zero field and in

condensed phase while its natural Ytterbium analogue is not.¹⁰ We then adopted such magnetic dilution strategy on its Yb^{III} analogue to produce SMM behavior in zero-applied magnetic field allowing the first isotopic enrichment investigation for a prolate Yb^{III} based-system.

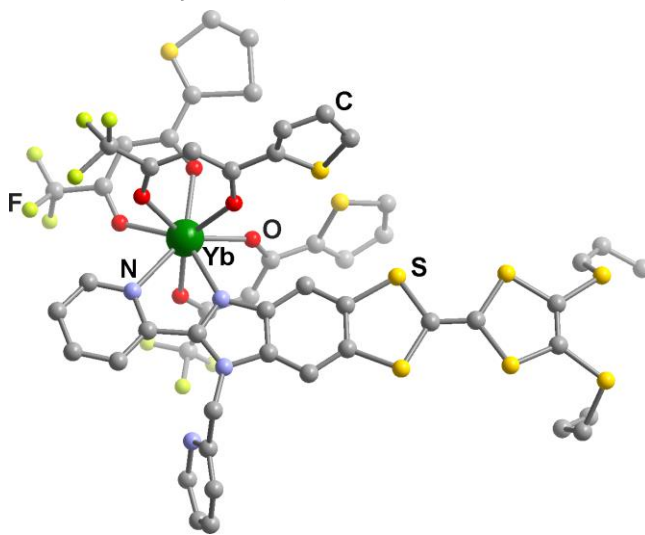


Figure 1. Molecular structure of **Yb**. Hydrogen atoms and n-hexane molecule of crystallization are omitted for clarity. Color code: carbon, grey; nitrogen, blue; oxygen, red; fluoride, green; sulphur, yellow and ytterbium, dark green

We briefly remind the main characteristics of $[Yb(tta)_3(L)] \cdot C_6H_{14}$ (here after called **Yb**) in the following lines. **Yb** crystallizes in the triclinic space group $P\bar{1}$ ($N^\circ 2$).¹⁰ **Yb** consists in one $[Yb(tta)_3(L)]$ complex in which $Yb^{III} N_2O_6$ coordination polyhedron adopts a distorted-square-antiprism symmetry (Table S1, Figure 1). Three tta^- anions and **L** provide six oxygen and two nitrogen atoms, respectively. MS-CASPT2 calculations showed that the Kramers ground state is constituted by $50\%|\pm 7/2\rangle + 30\%|\pm 5/2\rangle + 20\%|\pm 3/2\rangle$ with $g_z = 6.02$ and is separated from the first excited state by ~ 240 cm^{-1} (Table S5).¹⁰ Zero-field ac susceptibility measurements show that there is no out-of-phase signal at frequencies as high as 10 kHz down to 2 K. The diluted compounds, $^*Yb@Y$, are synthesized following an initial ratio $Yb(tta)_3 \cdot 2H_2O : Y(tta)_3 \cdot 2H_2O$ of 0.05:0.95.[†] These are isomorphous to **Yb**, as demonstrated by single crystal XRD unit cell determination (Table S2) and powder XRD (Figure S1), with the last being an insight of the purity of the sample. For the natural analogue, the ICP-OES analysis results in a ratio $Yb:Y = 0.06:0.94$. Natural ytterbium is constituted of various isotopes. Amongst them, the nuclear spin free ^{174}Yb ($I=0$, 32%) and

the nuclear spin active ^{173}Yb ($I=5/2$, 16%) isotopes have been used in order to synthesize the isotopically enriched diluted compounds $^{174}\text{Yb@Y}$ ($^{174}\text{Yb}_{0.1}\text{Y}_{0.9}(\text{tta})_3(\text{L})\cdot\text{C}_6\text{H}_{14}$) and $^{173}\text{Yb@Y}$ ($^{173}\text{Yb}_{0.07}\text{Y}_{0.93}(\text{tta})_3(\text{L})\cdot\text{C}_6\text{H}_{14}$) with the doping ratios obtained by ICP-OES. Magnetization curves at 2 K of the three diluted materials (Figure S2) have been compared to the one of **Yb** to estimate the dilution ratio $\text{Yb}:\text{Y}=0.05:0.95$ for **Yb@Y**, 0.05/0.95 for $^{173}\text{Yb@Y}$ and 0.11:0.89 for $^{174}\text{Yb@Y}$. It is worth to notice that g_z extracted from EPR spectrum of $^{174}\text{Yb@Y}$ ($g_z = 6.1$, Figure S3) is in agreement with MS-CASPT2 calculations.

Yb@Y behaves as a zero-field SMM with the emergence of a frequency dependent out-of-phase, χ_M'' , ac signal below 6 K (Figure 2b and S4), with a relaxation centered at ~ 500 Hz at 2 K. This shows that the SMM intrinsically exists in the condensed phase but that it is hindered by the weak dipolar intermolecular interactions. Isotopically enriched diluted samples with and without nuclear spin ($^{173}\text{Yb@Y}$ and $^{174}\text{Yb@Y}$ respectively) relax at very different frequencies at 2 K (5000 and 120 Hz) while they almost collapse on the natural product when the temperature rises (Figures 2 and S4). The average relaxation times can be estimated from the maximum on the χ_M'' vs. frequency curves for the three diluted samples and they are plotted on Figure 3. In the absence of external dc field, one should consider only Orbach, Raman and QTM relaxation processes with the latter, if present, coming from the hyperfine coupling.

$$\tau^{-1} = \underbrace{\tau_0^{-1} \exp\left(\frac{\Delta}{T}\right)}_{\text{Orbach}} + \underbrace{CT^n}_{\text{Raman}} + \underbrace{\tau_{\text{QTM}}^{-1}}_{\text{QTM}}$$

The expected n value for Kramers ions should be 9,¹¹ but the presence of both acoustic and optical phonons could lead to lower values comprised between 2 and 7¹² and in some cases even lower.¹³ The relaxation time of $^{173}\text{Yb@Y}$ is faster than $^{174}\text{Yb@Y}$ in the full studied temperature range (Figure 3). Such isotopic effect follows the trend already observed for isotopically enriched Dy-systems,^{6a,b,e,g} reinforcing the fact that slow relaxation is enhanced by suppression of dipolar (dilution) and hyperfine (isotopic enrichment) interactions for both oblate (Dy^{III})^{6a,b,e,g} and prolate (Yb^{III}) electronic distribution. One should consider however that they tend to merge with the temperature. At first, the only difference between 173 and 174 derivatives resides in the nuclear spin that is involved in QTM process for $^{173}\text{Yb@Y}$ and not for $^{174}\text{Yb@Y}$. The natural product **Yb@Y** falls in between the two pure isotopes whatever the temperature that matches the fact that the natural product is a mixture of various isotopes with and without nuclear spin. We mention however that the last spin active isotope (^{171}Yb , $I=1/2$, 14%) has not been investigated but is as abundant as ^{173}Yb . Then, the thermal variation of the relaxation time is simultaneously fitted for the three diluted samples with Orbach (Δ and τ_0) and Raman (C and n) shared parameters while different QTM (B_1) appears in $^{173}\text{Yb@Y}$ and **Yb@Y**. The best-fitted curves are represented on Figure 3 with $\Delta=33\pm 3$ K, $\tau_0=7\pm 4\times 10^{-8}$ s, $C=220\pm 54$ K⁻ⁿ s⁻¹, $n=1.6\pm 0.3$ and $\tau_{\text{QTM}}=3.237\pm 0.05\times 10^{-5}$ s for $^{173}\text{Yb@Y}$ and $\tau_{\text{QTM}}=3.30\pm 0.17\times 10^{-4}$ s for **Yb@Y**. One should mention two points : 1) fitting with Raman+QTM processes does not lead to convincing results (Figure S5) so Orbach contribution is included to account for the high temperature behavior 2) Raman exponent is very low and bottleneck might be invoked, however relaxation time should be longer in condensed phase that is not the case. At this stage, it is clear that Orbach parameters are isotopically independent. At the lowest studied temperatures, the Raman process (dashed purple line on Figure 3) dominates the relaxation mechanism in $^{174}\text{Yb@Y}$ (full red line on Figure 3) whereas

for $^{173}\text{Yb@Y}$ (full blue line on Figure 3) the relaxation is governed by the QTM (dashed blue line on Figure 3).

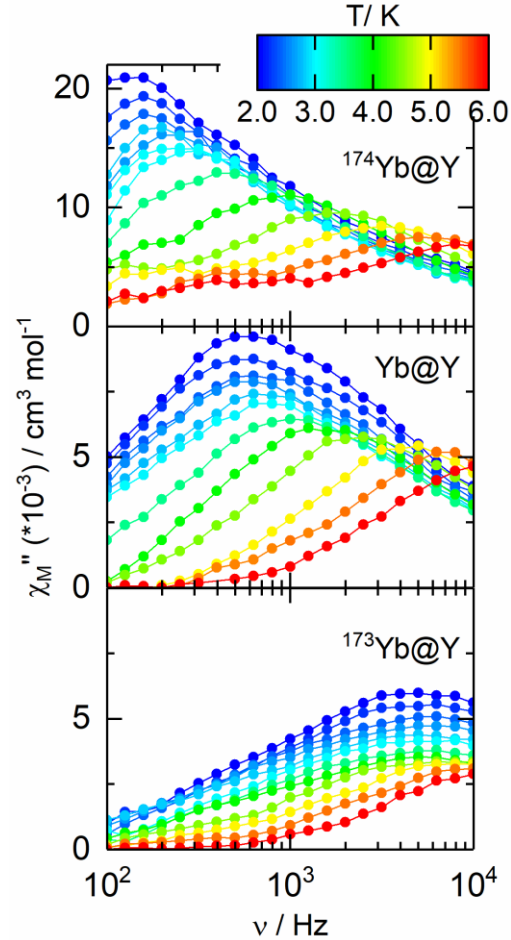


Figure 2. Frequency dependences of χ_M'' of $^{174}\text{Yb@Y}$, **Yb@Y** and $^{173}\text{Yb@Y}$ in zero external field in the 2-6 K temperature range.

Interestingly, even if **Yb** is not a zero-field SMM (Figure S6), an out-of-phase signal emerges at 2 K when a moderate external field of a few hundreds of Oe is applied (Figure S7). The relaxation speed (position of the maximum) does not significantly change with the applied magnetic field value but the amplitude of the relaxation does. This is monitored through the extended Debye model (SI, Table S3). The amount of magnetic moment that is involved in the relaxation grows (Table S3) with the magnetic field to reach almost 100% at 3 kOe, which means that all the isotopologues relax at the same frequency at such field. The relaxation time does not vary in a great extent but is slowest at 1 kOe (Table S3). At such optimum field, the thermal variation of the relaxation time is determined between 2 and 4 K (Figures S8 to S11 and Table S4) and almost superimpose to the zero-field data of $^{174}\text{Yb@Y}$ (Figure S12). This can be viewed as the effect of moderate external magnetic field that overtake the effects of both internal field and hyperfine coupling. One might see the in-field (~ 1 kOe or more) relaxation behavior in mononuclear complexes as a picture of the zero-field relaxation in diluted and isotopically enriched (with nuclear spin silent isotopes) derivative.

We have demonstrated the feasibility to generate a slow relaxation of the magnetic moment in zero external constant field in a system with prolate Yb^{III} from magnetic dilution. Indeed, the separation of mononuclear

Yb^{III} -based complexes in a solid matrix minimize the intermolecular interactions of dipolar and/or exchange origin that pull the relaxation time into a commonly accessible time window. This behavior can be further ameliorated with nuclear spin silent Yb^{III} isotope. In the present system, the combination of the two strategies slows down the relaxation time by a factor of at least 1000. In addition, the use of nuclear spin active isotopes has the opposite effect: it accelerates the relaxation processes in zero-field. We demonstrated that our strategy of enhancement of the magnetic performances of oblate Dy^{III} -based SMM can be extended to prolate Yb^{III} molecular systems. Indeed, this study constitutes the first investigation of the role of the hyperfine interaction on magnetization dynamics in zero field^{8b} of Yb^{III} -based SMMs. It evidences relaxation speeds of the order of one hundred time faster with nuclear spin active than with nuclear spin silent isotopes. Someone could ask if the global framework is applicable to other Yb^{III} -based system and is the nature of the Kramers doublet ground state essential to promote SMMs behaviors in Yb^{III} complexes.

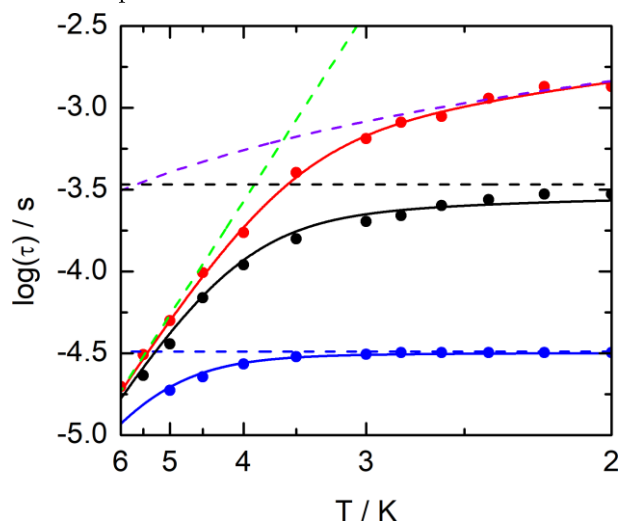


Figure 3. Temperature dependence of the relaxation times of the Yb@Y (black full circles) and its isotopologues $^{174}\text{Yb@Y}$ (red full circles) and $^{173}\text{Yb@Y}$ (blue full circles) in zero magnetic field and for the 2-6 K temperature range. Full lines correspond to the best fitted parameters (see text). Blue and black dashed lines represent the QTM contributions, green dashed line the Orbach contribution and the purple dashed line the Raman contribution to the magnetic relaxation processes.

ASSOCIATED CONTENT

Supporting Information

Additional magnetic data for Yb (Figures S6-11 and Tables S3-5), PXRD patterns (Figure S1), additional magnetic data for diluted samples (Figures S2-5), SHAPE analysis (Table S1), X-ray data (Table S2) and general procedures and materials section.

This material is available free of charge via the Internet at <http://pubs.acs.org>.

AUTHOR INFORMATION

Corresponding Author

E-mail: fabrice.pointillart@univ-rennes1.fr

E-mail: olivier.cador@univ-rennes1.fr

ORCID

Jessica Flores Gonzalez: 0000-0003-3722-8976

Boris Le Guennic: 0000-0003-3013-0546

Fabrice Pointillart: 0000-0001-7601-1927

Olivier Cador: 0000-0003-2064-6223

Notes

Isotopically enriched $^{\text{Yb}}(\text{tta})_3 \cdot 2\text{H}_2\text{O}$ ($x=173$ and 174) were synthesized by adding 2-thenyltrifluoroacetone (224 mg, 1.010 mmol) to 180 mL of distilled water. The mixture was stirred at 60°C and adjusted to pH 6-6.5 by dropwise of NH_4OH at 25%. Simultaneously, around 0.126 mmol of $^{\text{Yb}}\text{B}_2\text{O}_3$ (49.7 mg for $x=173$ and 50 mg for $x=174$) was dissolved in 130 μL of concentrated HCl (37%). After 30 min of stirring at 50°C , the resulting solution containing $^{\text{Yb}}\text{Cl}_3 \cdot 6\text{H}_2\text{O}$ (0.205 mmol) was diluted with 1 mL of water before being added to the former. The pH of the solution was adjusted to 7-7.5 during the stirring leading to a white precipitate of $\text{Yb}(\text{tta})_3 \cdot 2\text{H}_2\text{O}$ which was filtered.¹⁴ Yields $^{173}\text{Yb}(\text{tta})_3 \cdot 2\text{H}_2\text{O}$: 127.4 mg (58%); $^{174}\text{Yb}(\text{tta})_3 \cdot 2\text{H}_2\text{O}$: 123.5 mg (56%).

Synthesis of $[\text{Yb}(\text{tta})_3(\text{L})] \cdot \text{C}_6\text{H}_{14}$. L (24.4 mg, 0.04 mmol)¹⁵ and $\text{Yb}(\text{tta})_3 \cdot 2\text{H}_2\text{O}$ (34.9 mg, 0.04 mmol) were first dissolved separately in 8 mL of CH_2Cl_2 each, and then mixed and stirred during 15 min. Slow diffusion of *n*-hexane in the mother solution at room temperature in the dark led to red single crystals of Yb .

Synthesis of diluted samples $^{\text{Yb}}_{0.05}\text{Y}_{0.95}(\text{tta})_3(\text{L}) \cdot \text{C}_6\text{H}_{14}$. L (42.0 mg, 0.07 mmol) was dissolved in 15 mL of CH_2Cl_2 and a mixture of $^{\text{Yb}}(\text{tta})_3 \cdot 2\text{H}_2\text{O}$ (3 mg, 0.0035 mmol) and $\text{Y}(\text{tta})_3 \cdot 2\text{H}_2\text{O}$ (51.8 mg, 0.0665 mmol) in 10 mL of CH_2Cl_2 was mixed and stirred during 15 min. For crystallization, *n*-hexane was layered gently to the mother solution. Red prismatic single crystals were obtained after two weeks of diffusion and then slow evaporation at room temperature. Yields: Yb@Y : 54.2 mg (54%); $^{173}\text{Yb@Y}$: 72.2 mg (72%); $^{174}\text{Yb@Y}$: 70.9 mg (71%).

ACKNOWLEDGMENTS

This work was supported by the University of Rennes 1, the CNRS and the European Commission through the ERC-CoG 725184 MULTIPROSMM (project n. 725184). Université Bretagne Loire is thanked for the fellowship of J. F. G. at University of Manchester. Dr. F. Tuna is acknowledged for her help in recording EPR spectra.

REFERENCES

- (a) Rinehart, J. D.; Long, J. R. Exploiting single-ion anisotropy in the design of f-element single-molecule magnets. *Chem. Sci.* **2011**, 2, 2078-2085. (b) Sessoli, R.; Powell, A. K. Strategies towards single molecule magnets based on lanthanide ions. *Coord. Chem. Rev.* **2009**, 253, 2328-2341. (c) Woodruff, D. N.; Winpenny, R. E. P.; Layfield, R. A. Lanthanide Single-Molecule Magnets. *Chem. Rev.* **2013**, 113, 5110-5148. (d) Feltham, H. L. C.; Brooker, S. Review of purely 4f and mixed-metal nd-4f single molecule magnets containing only one lanthanide ion. *Coord. Chem. Rev.* **2014**, 276, 1-33. (e) Zhang, P.; Guo, Y.-N.; Tang, J. Recent advances in dysprosium-based single molecule magnets: Structural overview and synthetic strategies. *Coord. Chem. Rev.* **2013**, 257, 1728-1763. (f) Pointillart, F.; Le Guennic, B.; Cador, O.; Maury, O.; Ouahab, L. Lanthanide Ion and Tetrathiafulvalene-Based Ligand as a "Magic" Couple toward Luminescence, Single Molecule Magnets, and Magnetostructural Correlations. *Acc. Chem. Res.* **2015**, 48, 2834-2842. (g) Guo, F.-S.; Bar, A. K.; Layfield, R. A. Main Group Chemistry at the Interface with Molecular Magnetism. *Chem. Rev.* **2019**, 119, 14, 8479-8505. (h) Liddle, S. T.; van Slageren, J. Improving f-element single molecule magnets. *Chem. Soc. Rev.* **2015**, 44, 6655-6669.
- (a) Ishikawa, N.; Sugita, M.; Ishikawa, T.; Koshihara, S.-Y.; Kaizu, Y. Lanthanide Double-Decker Complexes Functioning as Magnets at the Single-Molecular Level. *J. Am. Chem. Soc.* **2003**, 125, 8694-8695. (b) Ishikawa, N.; Sugita, M.; Wernsdorfer, W. Quantum Tunneling of Magnetization in Lanthanide Single-

Molecule Magnets: Bis(phthalocyaninato)terbium and Bis(phthalocyaninato)dysprosium Anions. *Angew. Chem. Int. Ed.* **2005**, *44*, 2931-2935.

(3) (a) Goodwin, C. A. P.; Ortu, F.; Reta, D.; Chilton, N. F.; Mills, D. P. Molecular magnetic hysteresis at 60 kelvin in dysprosium. *Nature*, **2017**, *548*, 439-442. (b) Guo, F.-S.; Day, B. M.; Chen, Y.-C.; Tong, M.-L.; Mansikkamäki, A.; Layfield, R. A. A Dysprosium Metallocene Single-Molecule Magnet Functioning at the Axial Limit. *Angew. Chem. Int. Ed.*, **2017**, *56*, 11445-11449. (c) Guo, F.-S.; Day, B. M.; Chen, Y.-C.; Tong, M.-L.; Mansikkamäki, A.; Layfield, R. A. Magnetic hysteresis up to 80 kelvin in a dysprosium metallocene single-molecule magnet. *Science*, **2018**, *362*, 1400-1403. (d) McClain, K. R.; Gould, C. A.; Chakarawet, K.; Teat, S. J.; Groshens, T. J.; Long, J. R.; Harvey, B. G. High-temperature magnetic blocking and magneto-structural correlations in a series of dysprosium(III) metallocene single-molecule magnets. *Chem. Sci.* **2018**, *9*, 8492-8503.

(4) (a) Pointillart, F.; Cador, O.; Le Guennic, B.; Ouahab, L. Uncommon lanthanide ions in purely 4f single molecule magnets. *Coord. Chem. Rev.*, **2017**, *346*, 150-175. (b) AlDamen, M. A.; Cardona-Serra, S.; Clemente-Juan, J. M.; Coronado, E.; Gaita-Arino, A.; Martí-Gastaldo, C.; Luis, F.; Montero, O. Mononuclear Lanthanide Single Molecule Magnets Based on the Polyoxometalates $[\text{Ln}(\text{W}_3\text{O}_{18})_2]^{9-}$ and $[\text{Ln}(\beta_2\text{-SiW}_{11}\text{O}_{39})_2]^{12-}$ ($\text{Ln}^{\text{III}} = \text{Tb, Dy, Ho, Er, Tm, and Yb}$). *Inorg. Chem.*, **2009**, *48*, 3467-3479. (c) Liu, J.-L.; Yuan, K.; Leng, J.-D.; Ungur, L.; Wernsdorfer, W.; Guo, F.-S.; Chibotaru, L. F.; Tong, M.-L. A Six-Coordinate Ytterbium Complex Exhibiting Easy-Plane Anisotropy and Field-Induced Single-Ion Magnet Behavior. *Inorg. Chem.* **2012**, *51*, 8538-8544. (d) Soussi, K.; Jung, J.; Pointillart, F.; Le Guennic, B.; Lefevre, B.; Golhen, S.; Cador, O.; Guyot, Y.; Maury, O.; Ouahab, L. Magnetic and photo-physical investigations into Dy^{III} and Yb^{III} complexes involving tetrathiafulvalene ligand. *Inorg. Chem. Front.* **2015**, *2*, 1105-1117. (e) Sugita, M.; Ishikawa, N.; Ishikawa, T.; Koshihara, S.; Kaizu, Y. Static Magnetic-Field-Induced Phase Lag in the Magnetization Response of Tris(dipicolinato)lanthanides. *Inorg. Chem.* **2006**, *45*, 1299-1304. (f) Boulon, M. E.; Cucinotta, G.; Luzon, J.; Degl'Innocenti, C.; Perfetti, M.; Bernot, K.; Calvez, G.; Caneschi, A.; Sessoli, R. Magnetic Anisotropy and Spin-Parity Effect Along the Series of Lanthanide Complexes With DOTA. *Angew. Chem. Int. Ed.* **2013**, *52*, 350-354. (g) Yi, X.; Bernot, K.; Le Corre, V.; Calvez, G.; Pointillart, F.; Cador, O.; Le Guennic, B.; Jung, J.; Maury, O.; Placide, V.; Guyot, Y.; Roisnel, T.; Dai-guebonne, C.; Guillou, O. Unraveling the Crystal Structure of Lanthanide-Murexide Complexes: Use of an Ancient Complexometry Indicator as a Near-Infrared-Emitting Single-Ion Magnet. *Chem. Eur. J.* **2014**, *20*, 1569-1576. (h) Huang, W.; Xu, J.; Wu, D.; Huang, X.; Jiang, J. Rhodamine-based field-induced single molecule magnets in $\text{Yb}(\text{III})$ and $\text{Dy}(\text{III})$ series. *New J. Chem.* **2015**, *39*, 8650-8657. (i) Pedersen, K. S.; Dreiser, J.; Weihe, H.; Sibille, R.; Johannessen, H. V.; Sorensen, M. A.; Nielsen, B. E.; Sigrist, M.; Mutka, H.; Rols, S.; Bendix, J.; Piligkos, S. Design of Single-Molecule Magnets: Insufficiency of the Anisotropy Barrier as the Sole Criterion. *Inorg. Chem.* **2015**, *54*, 7600-7606. (j) Murugesu, M.; Richardson, P.; Marin, R.; Zhang, Y.; Gabidullin, B.; Ovens, J.; Moilanen, J. O. Asymmetric Ring Opening in Tetrazine-Based Ligand Affording a Tetranuclear Opto-Magnetic Ytterbium Complex. *Chem. Eur. J.* DOI: 10.1002/chem.202003556. (k) Brunet, G.; Marin, R.; Monk, M.-J.; Resch-Genger, U.; Gállico, D. A.; Sigoli, F. A.; Suturina, E. A.; Hemmer, E.; Murugesu, M. Exploring the Dual Functionality of an Ytterbium Complex for Luminescence Thermometry and Slow Magnetic Relaxation. *Chem. Sci.* **2019**, *10*, 6799-6808. (l) Chen, W.-B.; Zhong, L.; Zhong, Y.-J.; Zhang, Y.-Q.; Gao, S.; Dong, W. Understanding the Near-Infrared Fluorescence and Field-Induced Single-Molecule-Magnetic Properties of Dinuclear and One-Dimensional-Chain Ytterbium Complexes Based on 2-Hydroxy-3-Methoxybenzoic Acid. *Inorg. Chem. Front.* **2020**, *7*, 3136-3145. (m) Richardson, P.; Alves Gállico, D.; Ovens, J.; A. Sigoli, F.; Murugesu, M. Incorporation of a Nitrogen-Rich Energetic Ligand in a $\{\text{Yb}^{\text{III}}\}$ Complex Exhibiting Slow Relaxation of the Magnetisation under an Applied Field. *Dalton Trans.* **2020**, *49*, 10344-10348. (n) Fondo, M.; Corredoira-Vázquez, J.; García-Deibe, A. M.; Sanmartín-Matalobos, J.; Amozá, M.; Botas, A. M. P.; Ferreira, R. A. S.; Carlos, L. D.; Colacio, E. Field-Induced Slow Magnetic Relaxation and Luminescence Thermometry in a Mononuclear Ytterbium Complex. *Inorg. Chem. Front.* **2020**, *7*, 3019-3029.

(5) (a) Cosquer, G.; Pointillart, F.; Golhen, S.; Cador, O.; Ouahab, L. Slow Magnetic Relaxation in Condensed versus Dispersed Dysprosium(III) Mononuclear Complexes. *Chem. Eur. J.* **2013**, *19*, 7895-7905. (b) Habib, F.; Lin, P. H.;

Long, J.; Korobkov, I.; Wernsdorfer, W.; Murugesu, M. The Use of Magnetic Dilution To Elucidate the Slow Magnetic Relaxation Effects of a Dy^{III} Single-Molecule Magnet. *J. Am. Chem. Soc.* **2011**, *133*, 8830-8833.

(6) (a) Pointillart, F.; Bernot, K.; Golhen, S.; Le Guennic, B.; Guizouarn, T.; Ouahab, L.; Cador, O. Magnetic Memory in an Isotopically Enriched and Magnetically Isolated Mononuclear Dysprosium Complex. *Angew. Chem. Int. Ed.* **2015**, *54*, 1504-1507. (b) Kishi, Y.; Pointillart, F.; Lefevre, B.; Riobé, F.; Le Guennic, B.; Golhen, S.; Cador, O.; Maury, O.; Fujiwara, H.; Ouahab, L. Isotopically enriched polymorphs of dysprosium single molecule magnets. *Chem. Commun.* **2017**, *53*, 3575-3578. (c) Chen, Y.-C.; Liu, J.-L.; Wernsdorfer, W.; Liu, D.; Chibotaru, L. F.; Chen, X. M.; Tong, M.-L. Hyperfine-Interaction-Driven Suppression of Quantum Tunneling at Zero Field in a Holmium(III) Single-Ion Magnet. *Angew. Chem. Int. Ed.* **2017**, *56*, 4996-5000. (d) Huang, G.; Yi, X.; Jung, J.; Guillou, O.; Cador, O.; Pointillart, F.; Le Guennic, B.; Bernot, K. Optimization of Magnetic Relaxation and Isotopic Enrichment in Dimeric Dy^{III} Single-Molecule Magnets. *Eur. J. Inorg. Chem.* **2018**, 326-333. (e) Tesi, L.; Salman, Z.; Cimatti, I.; Pointillart, F.; Bernot, K.; Mannini, M.; Sessoli, R. Isotope effects on the spin dynamics of single-molecule magnets probed using muon spin spectroscopy. *Chem. Commun.* **2018**, *54*, 7826-7829. (f) Ortu, F.; Reta, D.; Ding, Y.-S.; Goodwin, C. A. P.; Gregson, M. P.; McInnes, E. J. L.; Wippeny, R. E. P.; Zheng, Y.-Z.; Liddle, S. T.; Mills, D. P.; Chilton, N. F. Studies of hysteresis and quantum tunnelling of the magnetisation in dysprosium(III) single molecule magnets. *Dalton Trans.* **2019**, *48*, 8541-8545. (g) Flores Gonzalez, J.; Pointillart, F.; Cador, O. Hyperfine coupling and slow magnetic relaxation in isotopically enriched Dy^{III} mononuclear single-molecule magnets. *Inorg. Chem. Front.* **2019**, *6*, 1081-1086.

(7) (a) Moreno-Pineda, E.; Damjanović, M.; Fuhr, O.; Wernsdorfer, W.; Ruben, M. Nuclear Spin Isomers: Engineering a $\text{Et}_2\text{N}[\text{DyPc}]$ Spin Qudit. *Angew. Chem. Int. Ed.* **2017**, *56*, 9915-9919. (b) Moreno-Pineda, E.; Taran, G.; Wernsdorfer, W.; Ruben, M. Quantum Tunnelling of the Magnetisation in Single-Molecule Magnet Isotopologue Dimers. *Chem. Sci.* **2019**, *10*, 5138-5145.

(8) (a) Thiele, S.; Balestro, F.; Ballou, R.; Klyatskaya, S.; Ruben, M.; Wernsdorfer, W. Electrically driven nuclear spin resonance in single-molecule magnets. *Science* **2014**, *344*, 1135-1138. (b) Pedersen, K. S.; Ariciu, A.-M.; McAdams, S.; Weihe, H.; Bendix, J.; Tuna, F.; Piligkos, S. Toward Molecular 4f Single-Ion Magnet Qubits. *J. Am. Chem. Soc.* **2016**, *138*, 5801-5804. (c) Godfrin, C.; Ferhat, A.; Ballou, R.; Klyatskaya, S.; Ruben, M.; Wernsdorfer, W.; Balestro, F. Operating Quantum States in Single Magnetic Molecules: Implementation of Grover's Quantum Algorithm. *Phys. Rev. Lett.* **2017**, *119*, 187702.

(9) da Cunha, T. T.; Jung, J.; Boulon, M.-E.; Campo, G.; Pointillart, F.; Pereira, C. L. M.; Le Guennic, B.; Cador, O.; Bernot, K.; Pineider, F.; Golhen, S.; Ouahab, L. Magnetic Poles Determinations and Robustness of Memory Effect upon Solubilization in a Dy^{III} -Based Single Ion Magnet. *J. Am. Chem. Soc.* **2013**, *135*, 16332-16335.

(10) Jung, J.; da Cunha, T. T.; Le Guennic, B.; Pointillart, F.; Pereira, C. L. M.; Luzon, J.; Golhen, S.; Cador, O.; Maury, O.; Ouahab, L. Magnetic Studies of Redox-Active Tetrathiafulvalene-Based Complexes: Dysprosium vs. Ytterbium Analogues. *Eur. J. Inorg. Chem.* **2014**, 3888-3894.

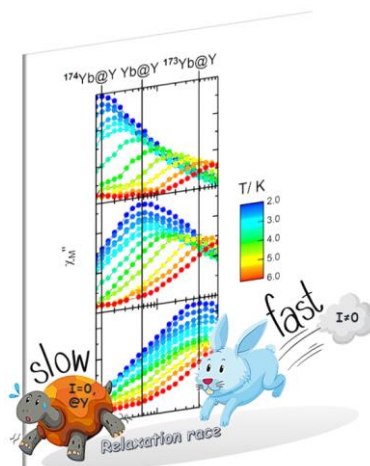
(11) Abragam, A.; Bleaney, B. *Electron Paramagnetic Resonance of Transition Ions*, Clarendon Press, Oxford, 1970.

(12) (a) Singh, A.; Shrivastava, K. N. Optical-acoustic two-phonon relaxation in spin systems. *Phys. Status Solidi B* **1979**, *95*, 273-277. (b) Shrivastava, K. N. Theory of Spin-Lattice Relaxation. *Phys. Status Solidi B* **1983**, *177*, 437-458.

(13) (a) Evans, P.; Reta, D.; Whitehead, G. F. S.; Chilton, N. F.; Mills, D. P. Bis-Monophospholyl Dysprosium cation Showing Magnetic Hysteresis at 48 K. *J. Am. Chem. Soc.* **2019**, *141*, 19935-19940. (b) Reta, D.; Chilton, N. F. Uncertainly estimates for magnetic relaxation times and magnetic relaxation parameters. *Phys. Chem. Chem. Phys.* **2019**, *21*, 23567-23575.

(14) Voloshin, A. I.; Shavaleev, N. M.; Kazakov, V. P. Chemiluminescence of praseodymium (III), neodymium (III) and ytterbium (III) β -diketonates in solution excited from 1,2-dioxetane decomposition and singlet-singlet energy transfer from ketone to rare-earth β -diketonates. *J. Lumin.* **2000**, *91*, 49-58.

(15) Cosquer, G.; Pointillart, F.; Jung, J.; Le Guennic, B.; Golhen, S.; Cador, O.; Guyot, Y.; Brenier, A.; Maury, O.; Ouahab, L. Alkylation Effects in lanthanide Complexes Involving Tetrathiafulvalene Chromophores: Experimental and Theoretical Correlation between Magnetism and Near-Infrared Emission. *Eur. J. Inorg. Chem.* **2014**, 69-82.



Isotopic enrichment and magnetic dilution are combined to generate an unprecedented zero-field single-molecule magnet behavior in an Ytterbium based complex.